Introduction/Framing

Understanding the interrelated dynamics of size- and -abundance based dimensions of biodiversity is key to understanding biodiversity change in the Anthropocene. Total abundance - i.e. the total number of individual organisms present in a system - and size-based currencies, such as the total biomass or total metabolic flux ("energy use") of a system, are intertwined, but nonequivalent, measures of biological function. Abundance is more closely tied to species-level population dynamics, while size-based metrics more directly reflect assemblage-level resource use and contributions to materials fluxes at the broader ecosystem scale (Morlon et al. 2009, Dornelas et al. 2011, Connolly et al. 2005, White et al. 2007). While these currencies are naturally linked (Morlon et al. 2009, Henderson and Magurran 2010), changes in size composition can decouple the dynamics of one currency from another (Ernest et al. 2009, Dornelas et al. 2011, White et al. 2004, 2007, Yen et al. 2017). This can mean that intuition from one currency may be misleading about others; a trend in numerical abundance might mask something else going on with biomass (White et al. 2004). Changes in size composition strong enough to decouple currencies may be symptomatic of important changes in ecosystem status- e.g. abundance-biomass comparison curves (Petchey and Belgrano 2010); size-biased extinctions (Young et al. 2016, Smith et al. 2018). This underscores the need to understand how these dynamics are playing out in the Anthropocene (Fisher et al. 2010).

At the **community scale**, changes in the relationship between size and abundance tells us about important functional shifts. This is the scale at which ecological processes (i.e. compensatory dynamics, niche tracking, functional replacement) come into play - in contrast to population or global trends (White et al. 2007, Dornelas et al. 2014, McGill et al. 2015). To the extent that size is a proxy for other functional traits, changes or consistency in the community-level size structure (individiual size distribution, ISD) over time may reflect processes related to niche structure (White et al. 2007, Petchey and Belgrano 2010). Strong size shifts can decouple the relationship between abundance and biomass. In aquatic systems, such changes in the scaling between abundance and biomass often signal ecosystem degradation (Kerr and Dickie 1AD, Warwick and Clarke 1994 and refs therein, Petchey and Belgrano 2010). Compensatory shifts in the size structure can buffer community function (in terms of biomass or energy use) against changes in abundance (Ernest et al. 2009, White et al. 2004, Terry and Rowe 2015). Consistency in the size structure may maintain the relationship between size- and -abundance based currencies, even as species composition, total abundance, and total biomass/total energy use fluctuate over time, which can reflect consistency in the niche structure over time (Holling 1992).

It is important to improve our understanding of these dynamics for terrestrial animal communities in particular. In contrast to terrestrial trees and aquatic systems (Kerr and Dickie 1AD, White et al. 2007), how the relationship between size and abundance changes over time, and the consequences of these changes for ecosystem-level properties, remain relatively unknown for terrestrial animals (but see White et al. (2004)). Terrestrial animal communities exhibit size structure (Thibault et al. 2011, Ernest 2005), and case studies have demonstrated that size shifts can either decouple N from E for terrestrial animals (White et al. 2004, Yen et al. 2017), but not always (Hernández et al. 2011). Establishing generalities in these dynamics is especially pertinent in the Anthropocene, as these communities are experiencing extensive and potentially size-structured change, with implications at community, ecosystem, and global scales (Young et al. 2016, Schmitz et al. 2018).

Macroecological-scale synthesis on the interrelated dynamics of the ISD, total abundance, and community function for terrestrial animals has been constrained by 1) a lack of community-level size and abundance timeseries data for these systems (Thibault et al. 2011, White et al. 2007), and 2) appropriate statistical methods for relating change in the size structure to changes in abundance and function (Thibault et al. 2011, Yen et al. 2017). In contrast to aquatic and forest systems, most long-term surveys of animal communities do not collect data on individuals' *sizes* across a full community (with the exception of small mammal studies, which have made major contributions to our understanding of the dynamics of size, abundance, and function for these systems; (White et al. 2004, Ernest 2005, Hernández et al. 2011, Kelt et al. 2015)). Global, continental, or population-wide studies capture different phenomena [White et al. (2007); this is a nod to a few studies looking at the size structure *across britain* or something]. The ISDs for terrestrial animals, and specifically for determinate growing taxa (e.g. mammals, birds), are often complex, multimodal distributions

(Holling 1992, Thibault et al. 2011, Ernest 2005, Yen et al. 2017), and less statistically tractable than the power-law ISDs found in aquatic and tree systems [Kerr and Dickie (1AD); White et al. (2007); more]. Quantifying change in the size structure, and relating this to change in community-wide abundance and function, is not as straightforward as computing and comparing slopes. As a result, we do not have a general understanding of either 1) the extent to which changes in the ISD decouple the community-level dynamics of abundance, biomass, and energy use in these systems, or of 2) the underlying changes in community structure that account for these effects.

Here, we begin to address this gap by exploring how temporal changes in species composition and the size spectrum modulate the relationship between total abundance, energy, and biomass for communities of North American breeding birds. We used allometric scaling to estimate community size and abundance data for the North American Breeding Bird Survey, and evaluated how changes in total abundance, biomass, and energy use have co-varied from 1988-2018. Specifically, we examined: 1) How often do these currencies change together vs. have decoupled dynamics?; 2) What are the dominant directions and magnitudes of the overall change and any decoupling between the currencies? We also examined how these changes differ between core species and the whole-community (i.e. including transients), which currently comes completely out of left field in this introduction (sorry!).

Methods

Bird abundance data

We used data from the Breeding Bird Survey (Sauer et al. 2013) to compare community attributes along each route between the 5-year periods from 1988-1992 and 2014-2018. We take the route to be the "community" scale [Thibault et al. (2011); others]. BBS (BBS methods background). We filtered the data to remove taxa that are poorly sampled through these methods, following (literally everyone). We accessed the data, and performed this preliminary cleaning and filtering, using the R package `MATSS` (Ye et al. 2020).

We used a discrete time-period comparison (as opposed to continuous-time over the full timeseries) to simplify comparisons between temporal turnover in the size structure - which are complex, multidimensional distributions - and changes in community-wide total abundance, biomass, and energy use. We acknowledge that a continuous-time perspective may be better equipped to detect nonlinear dynamics (Macgregor et al. 2019) and account for artefacts related to the selected beginning and ending dates (Cusser et al. 2020, Bahlai et al. 2021). Developing continuous-time methods for analyzing community distributions such as the size spectrum is an important and ongoing area of methodological development (e.g. Yen et al. (2017)).

We used 5-year periods to account for sampling accumulation effects in characterizing the bird community in each time period (White 2004). We used the same begin and end dates for all routes in the analysis so as to have a consistent window. We explored the number of routes in the dataset with complete sampling coverage for two five-year "begin" and "end" periods with start dates ranging from 1970 to 1990 and end dates ranging from 2000 to 2018, and selected beginning and ending dates of 1988 and 2018 so as to obtain a large number of routes from diverse bird conservation regions, and span a relatively long window of time (could ref Cusser et al. (2020) there). This yielded 528 routes. å

Estimated size data

BBS contains abundances for all species along a route in each year, but does not include measurements of individual body size. We generated body size estimates for individual birds assuming that intraspecific size distributions are normally distributed around a species' mean body size (following Thibault et al. (2011)). Using records of species' mean and standard deviation body sizes from (**???**), we drew individuals' body sizes from the appropriate normal distributions. For species for which there was not a standard deviation recorded in (**???**) (185 species affected, of 421 total), we estimated the standard deviation based on an allometric scaling relationship between mean and standard deviation in body mass ($log(variance) =$

$-5.273 + (log(mass) * 1.995))$; model R2 .86; see also Thibault et al. (2011)). For species with multiple records in (**???**), we used the mean mean and standard deviation body sizes across all records (averaging across sexes, subspecies, and records from different locations). We performed this averaging after estimating any missing standard deviation measurements. For each individual bird observed, we estimated metabolic rate as $10.5 * (mass^{.713})$ (**???**, **???**, Fristoe 2015). For each route in a given year, we compute total energy use, total biomass, and total abundance by summing over all individuals observed on that route in that year. This method does not incorporate intraspecific variation in body size across geographies or over time (**???**, Gardner et al. 2011). However, it makes it possible to conduct macroecological studies of avian size distributions at a spatial and temporal scale that would otherwise be impossible (Thibault et al. 2011).

Comparing ISDs over time

For each route, we used two approaches to test whether the ISD for 1988-1992 is significantly different from the one for 2014-2018. First, we used a Kolmogorov-Smirnov test on the vector of masses for the beginning and end time periods. Second, we performed bootstrap resampling to test whether the observed degree of dissimilarity between the two time periods exceeded that which would be expected if the probability of an individual being a particular size did not depend on which time period it was observed in (I believe following Ernest (2005)). From the pool of all individuals observed in both timeperiods, we re-assigned individuals to each time period at random and without replacement, and computed the Kolmogorov-Smirnov test statistic D comparing the resulting vectors of masses for each time period. We repeated this 500 times, and calculated the percentile score and standardized effect size (SES) of Kolmogorov-Smirnov D for the *observed* ISDs compared to the distribution of Ds from the bootstrap samples. Percentile scores > 95 and SES > 2 correspond to an observed pair of ISDs significantly more dissimilar than the bootstrap samples.

For an intuitive measure of the *magnitude* of change in the ISD over time, we compute an overlap measure (see Read et al. (2018) for this measure applied to species-level body size distributions). We characterize the ISD as a smooth function by fitting a Gaussian mixture model (to logarithm of mass, up to 15 Gaussians, select best using BIC, all following Thibault et al. (2011)). We evaluate the density function of the GMM at points for a size range from 0-exp(15), which covers the range of sizes in this dataset with ample padding on each side. We rescale the density function so the total area under the ISD is 1. We calculate the overlap between two ISDs as the sum of the minimum density at each evaluation point. This ranges from 0 (no overlap) to 1 (complete overlap) (Read et al. 2018).
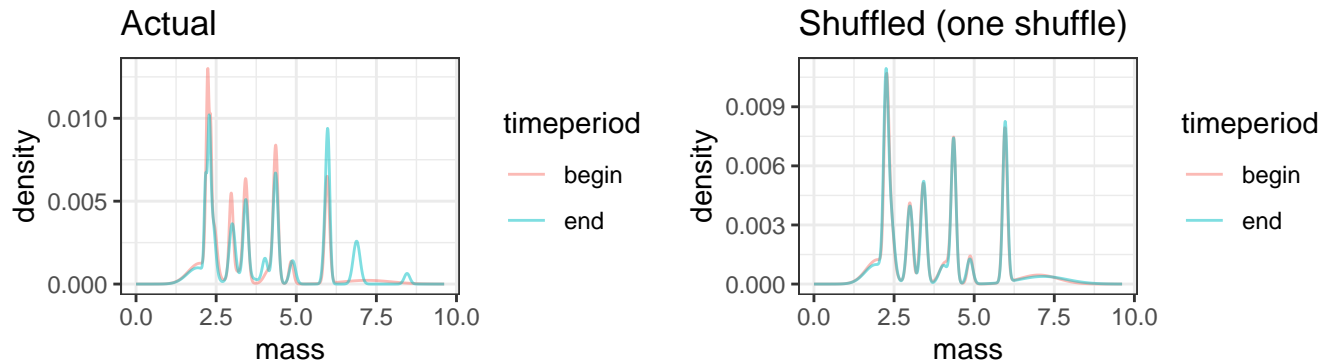
For this site (ZIMOVIA STRT, ALASKA), the KS test p value is 0. The observed test statistic has a percentile of 1 and SES of 11.58 compared to 500 bootstraps. The observed ISDs have an overlap of 0.81.

# Decoupling of dynamics in total abundance, biomass, and energy use over time

Sims

To test whether change in biomass or energy use deviates from the change in abundance, we can't just compare the slopes for total energy, total biomass, and total abundance to each other. This is because the three different currencies are on radically different scales of measurement. We also can't rescale using the usual methods (e.g. scale to mean 0/sd 1, sqrt transform Dornelas et al. (2014); Gotelli et al. (2017)) because these destroy information about the range of variability within a single currency. Instead, we test whether the observed change in biomass or energy use differs from the change that we would expect given observed changes in community-wide abundance, but with *no change* in the ISD from beginning to end.

Figures and functions walking through this procedure are at https://github.com/diazrenata/redwing/blob/resim-cleanup/aspirational_structure/methods_vignettes/change_over_time/02_01_change_over_time_sims.md but they're a little rough.

We simulate change in total energy and total biomass under "no change in ISD" and "observed change in ISD" scenarios. We use the GMM smooth procedure described above to characterize a "sampling GMM" for each time period. The "sampling GMM" is a probability density function with the probability of observing an individual of a given mass across the spectrum of possible masses. Sampling `$mass` with probability `$density` is a random number generator for sizes. We then *re draw* individuals for each year under different scenarios. First, we draw individuals for each year using the actual ISD for that time period (so the "begin" ISD for 1988-1992 and the "end" ISD for 2014-2018). Second, we draw individuals for each year, but using the "begin" ISD for all years, to estimate community properties if the ISD had not changed from beginning to end. We compute the total energy use and total biomass for each year under each scenario.

Note that we pool individuals within a time period to create the ISD, to smooth out species accumulation, but we draw individuals and compute total energy and biomass year-by-year, instead of pooling individuals over the whole time period, to capture interannual, intratimeperiod variation in total abundance (which propagates to total energy use and total biomass).
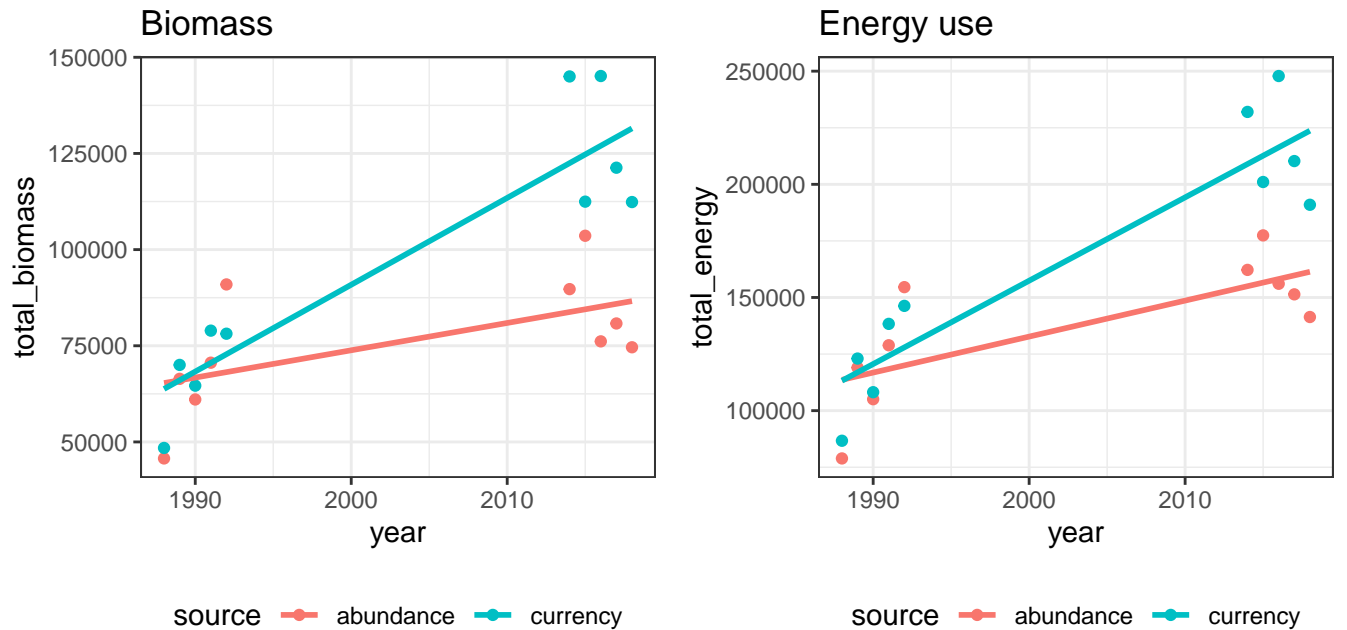
Here, the "abundance" line (red) reflects change in total biomass expected due only to changes in abundance. The "currency" line reflects change in total biomass due to change in abundance *and* observed change in the size structure. Deviations in slope between the red and blue lines reflect change driven by the ISD. Note that the lines here are crude linear model smooths and not really suitable for inference, just visualization.

Testing change

We use Bayesian linear models to test whether change in the ISD decouples the dynamics of total biomass/total energy use from that which would be expected due to change in abundance.

We evaluate change at the route level, because we care most about the decoupling of slopes for "currency" and "abundance" at the route level.

For each currency for each route, we fit 3 models:

1. `total_biomass ~ timeperiod * scenario`: I call this one "full"; this model has a slope for abundance, and an offset resulting in a *different* slope for currency
2. `total_biomass ~ timeperiod`: I call this one "nosource"; this one has a slope for abundance but not a different slope for currency
3. `total_biomass ~ 1`: Intercept-only model, no change over time.

We fit as Gaussians with default priors, run for 8000 iterations. We used LOO-crossvalidation (as implemented in `rstanarm::loo`) to select the best-fitting model as the simplest model with an ELPD within 1 SE of the best-fitting model, using `reloo` to correct for outliers.

If the best-fitting model does not include the scenario term (i.e. "currency" separate from "abundance"), it means that the change in the ISD does not ~significantly decouple the dynamics of total energy/biomass from that which is driven by changes in abundance. If there is no **timeperiod** term, it means that there's not a ~significant change begin-end.

We fit these models for `total_biomass` and `total_energy` for all routes. For each currency, we tallied: 1. How often the best model includes the "source" term (meaning there's a decoupling); 2. how often there's a timeperiod but no source term (meaning there's change over time, but that biomass/energy use do not diverge from abundance); 3. how often there's no timeperiod term (meaning no ~significant change begin to end).

For the example site we've been working with, here are the winning models. Both biomass and energy select the "full" model, meaning there's a decoupling between the size-based currencies and just abundance.

```
## # A tibble: 2 x 3
##   simtype currency model
##   <chr>   <chr>    <chr>
## 1 actual  biomass  tb_stanlm_full
## 2 actual  energy   te_stanlm_full
```

For models with slope and/or offset terms, we extracted estimates for the slope for abundance, and the offset for currency, to examine the magnitude and direction of change and decoupling. We tallied how often the abundance slope was positive or negative (how often the 95% CI for the timeperiod term is $>/< 0$) and how often the offset for currency is positive or negative (how often the 95% CI for the timeperiod:source term is $>/< 0$). Positive offsets mean that the change in biomass/energy use is less negative than change in abundance; negative offsets mean that the currency is more negative.

For the "actual" sims, here are the parameter estimates for the slope and offset. Thick bars are the 95% and thin bars are the 99% CIs. For both energy and biomass, the abundance-driven trajectory is an increase, but it's less of a strong increase for biomass. For both, the currency-driven offset is also an increase, meaning that the change in the ISD caused biomass to increase more than we expect it to just because of the increase in abundance.
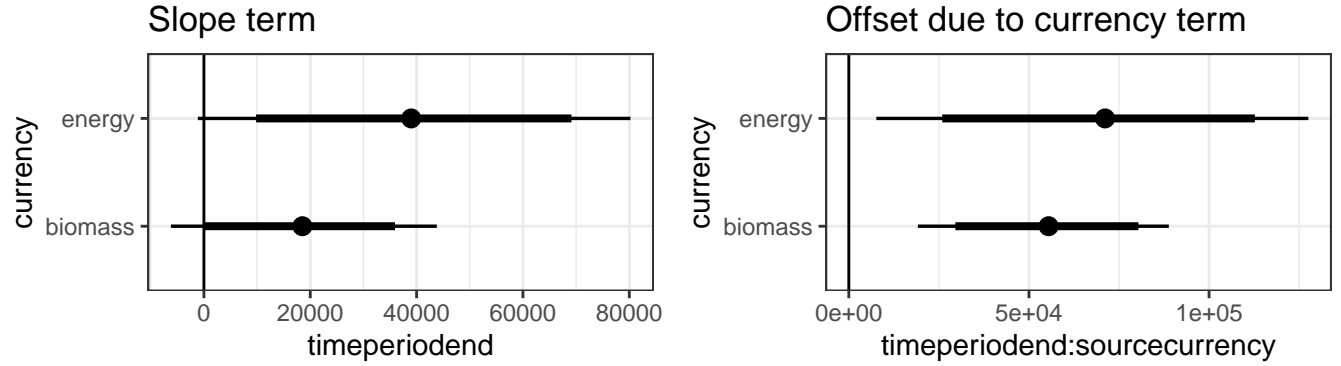
Miscellany

These probably belong in figure captions/supplements, not as the methods.

Relating change in the ISD to decoupling

The ISD may change without resulting in a detectable decoupling of the dynamics of biomass/energy use and abundance at the whole-system level, if the change in the ISD is relatively ~balanced above and below the mean body size. We tested whether communities with a decoupling showed greater change in the ISD than systems that did not, using a linear model of the form `isd_overlap ~ winning_model_type`. We also tested the extent to which change in mean body size was linked to change in the ISD using a quadratic model of the form `isd_overlap ~ logratio_mean_body_size + logratio_mean_body_size ^ 2`. We fit a quadratic model because we expected there to be a unimodal relationship, because high ISD overlap constrains there to be very little change in mean body size.

Core-transient

Because core and transient species may have different dynamics, we ran this pipeline on whole communities, and using just core species (those present in $>= 2/3$ of timesteps).

Results

Change in the ISD begin-to-end

"Significance"

In 523 of 528 routes, the KS-test finds a significant difference in the raw ISDs begin-to-end. In 523 of 528, the percentile score of the KS-test statistic (relative to the bootstrap model) is greater than .95. In 523 of 528, the SES > 2. We proceed as though the "begin" and "end" ISDs are always "significantly" different, and investigate the magnitude and consequences of these differences.

Magnitude
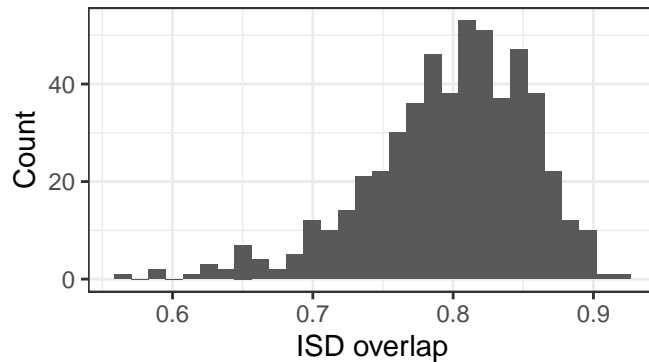

```
##    Min. 1st Qu.  Median    Mean 3rd Qu.    Max.
##  0.5584  0.7634  0.8056  0.7973  0.8402  0.9143
```

For most sites, these significant differences translate into about 80% overlap/20% change in the distribution of density under the ISD - similar to the degree of change in the example shown above.

Change in abundance and function

Model tallies

```
## # A tibble: 6 x 6
## # Groups:   currency [2]
##   currency model                 n percent model_name    omodel_name
##   <chr>    <chr>             <int>   <dbl> <chr>         <ord>
## 1 Biomass  tb_stanlm_full      178    33.7 Decoupling    Decoupling
## 2 Biomass  tb_stanlm_nosource  208    39.4 Slope         Slope
## 3 Biomass  tb_stanlm_notime    142    26.9 Intercept-only Intercept-only
## 4 Energy   te_stanlm_full       76    14.4 Decoupling    Decoupling
## 5 Energy   te_stanlm_nosource  290    54.9 Slope         Slope
## 6 Energy   te_stanlm_notime    162    30.7 Intercept-only Intercept-only
```

For 69 percent (for energy use) and 73 percent (for biomass) of routes, there is a detectable change in abundance and/or one of the currencies from begin to end.

For 14 percent (for energy) and 34 percent (for biomass) of routes, there is a *decoupling* of the dynamics of the currency from what would be expected given change in abundance alone.

Direction of change in abundance

```
## # A tibble: 2 x 3
##   currency prop_increasing prop_decreasing
##   <chr>              <dbl>           <dbl>
## 1 biomass            0.228           0.578
## 2 energy             0.270           0.653
```

For about 60% of models *with a change beginning to end*, abundance is decreasing. Note that the number that are increasing vs. decreasing can sum to less than 1 if there are models with an interaction in which the abundance-slope is over 0, but the currency offset is nonzero.

Direction of offset due to ISD

```
## # A tibble: 2 x 4
##   currency percent_currency_above_abund percent_currency_belo~ n_with_interacti~
##   <chr>                           <dbl>                  <dbl>             <int>
## 1 biomass                         0.803                  0.197               178
## 2 energy                          0.75                   0.237                76
```

For models with a currency offset, nearly **80% of the time** that offset is towards the currency-slope being less negative than for abundance.

Energy

Biomass
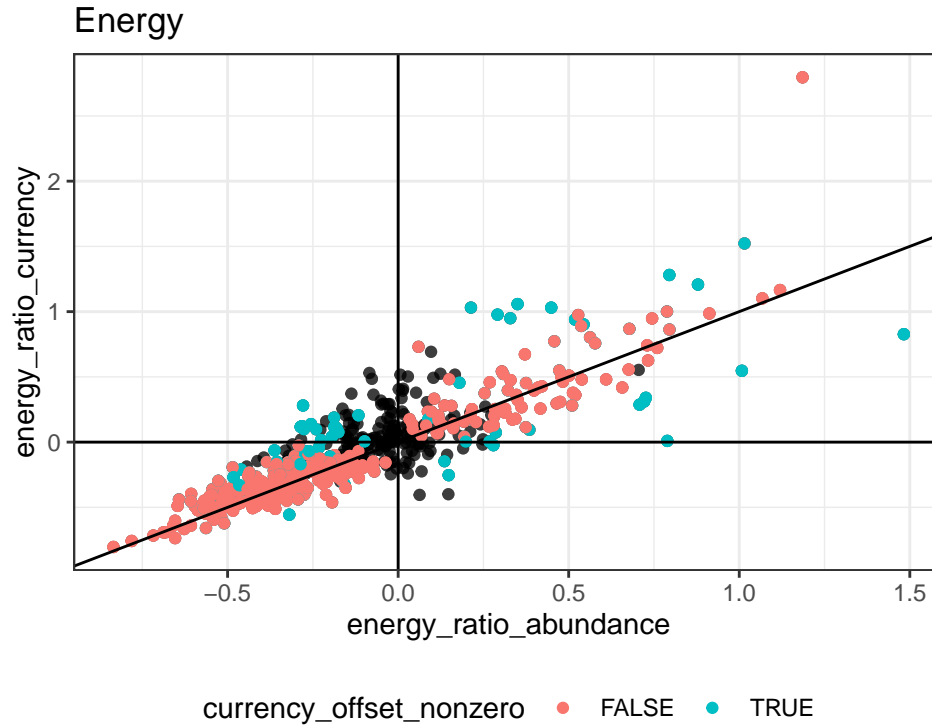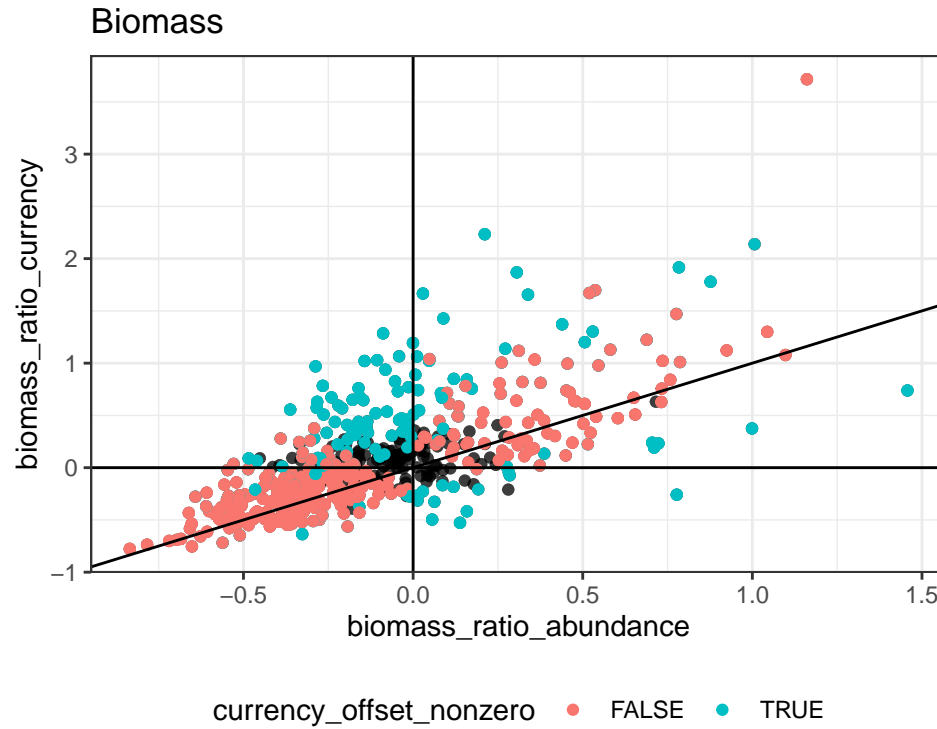
Relating change in the ISD to decoupling

There's a lot of change in the ISD that doesn't translate into decoupling.

Core-transient

Everything stays the same **except for** the 80%.

Highly sampled BCRs

Totally the same.

References

Bahlai, C. A., E. R. White, J. D. Perrone, S. Cusser, and K. Stack Whitney. 2021. The broken window: An algorithm for quantifying and characterizing misleading trajectories in ecological processes. Ecological Informatics 64:101336.

Connolly, S. R., T. P. Hughes, D. R. Bellwood, and R. H. Karlson. 2005. Community Structure of Corals and Reef Fishes at Multiple Scales. Science 309:1363–1365.

Cusser, S., C. Bahlai, S. M. Swinton, G. P. Robertson, and N. M. Haddad. 2020. Long-term research avoids spurious and misleading trends in sustainability attributes of no-till. Global Change Biology 26:3715–3725.

Dornelas, M., N. J. Gotelli, B. McGill, H. Shimadzu, F. Moyes, C. Sievers, and A. E. Magurran. 2014. Assemblage Time Series Reveal Biodiversity Change but Not Systematic Loss. Science 344:296–299.

Dornelas, M., D. A. T. Phillip, and A. E. Magurran. 2011. Abundance and dominance become less predictable as species richness decreases. Global Ecology and Biogeography 20:832–841.

Ernest, S. K. M. 2005. Body size, energy use, and community structure of small mammals. Ecology 86:1407–1413.

Ernest, S. K. M., E. P. White, and J. H. Brown. 2009. Changes in a tropical forest support metabolic zero-sum dynamics. Ecology Letters 12:507–515.

Fisher, J. A. D., K. T. Frank, and W. C. Leggett. 2010. Dynamic macroecology on ecological time-scales. Global Ecology and Biogeography 19:1–15.

Fristoe, T. S. 2015. Energy use by migrants and residents in North American breeding bird communities. Global Ecology and Biogeography 24:406–415.

Gardner, J. L., A. Peters, M. R. Kearney, L. Joseph, and R. Heinsohn. 2011. Declining body size: A third universal response to warming? Trends in Ecology & Evolution 26:285–291.

Gotelli, N. J., H. Shimadzu, M. Dornelas, B. McGill, F. Moyes, and A. E. Magurran. 2017. Community-level regulation of temporal trends in biodiversity. Science Advances 3:e1700315.

Henderson, P. A., and A. E. Magurran. 2010. Linking species abundance distributions in numerical abundance and biomass through simple assumptions about community structure. Proceedings of the Royal Society B: Biological Sciences 277:1561–1570.

Hernández, L., J. W. Laundré, A. González-Romero, J. López-Portillo, and K. M. Grajales. 2011. Tale of two metrics: Density and biomass in a desert rodent community. Journal of Mammalogy 92:840–851.

Holling, C. S. 1992. Cross-Scale Morphology, Geometry, and Dynamics of Ecosystems. Ecological Monographs 62:447–502.

Kelt, D. A., J. R. Aliperti, P. L. Meserve, W. B. Milstead, M. A. Previtali, and J. R. Gutierrez. 2015. Energetic compensation is historically contingent and not supported for small mammals in South American or Asian deserts. Ecology 96:1702–1712.

Kerr, S. R., and L. M. Dickie. 1AD. The Biomass Spectrum: A Predator-Prey Theory of Aquatic Production. Columbia University Press.

Macgregor, C. J., J. H. Williams, J. R. Bell, and C. D. Thomas. 2019. Moth biomass increases and decreases over 50 years in Britain. Nature Ecology & Evolution 3:1645–1649.

McGill, B. J., M. Dornelas, N. J. Gotelli, and A. E. Magurran. 2015. Fifteen forms of biodiversity trend in the Anthropocene. Trends in Ecology & Evolution 30:104–113.

Morlon, H., E. P. White, R. S. Etienne, J. L. Green, A. Ostling, D. Alonso, B. J. Enquist, F. He, A. Hurlbert, A. E. Magurran, B. A. Maurer, B. J. McGill, H. Olff, D. Storch, and T. Zillio. 2009. Taking species abundance distributions beyond individuals. Ecology Letters 12:488–501.

Petchey, O. L., and A. Belgrano. 2010. Body-size distributions and size-spectra: Universal indicators of ecological status? Biology Letters 6:434–437.

Read, Q. D., J. M. Grady, P. L. Zarnetske, S. Record, B. Baiser, J. Belmaker, M.-N. Tuanmu, A. Strecker, L. Beaudrot, and K. M. Thibault. 2018. Among-species overlap in rodent body size distributions predicts species richness along a temperature gradient. Ecography 41:1718–1727.

Sauer, J. R., W. A. Link, J. E. Fallon, K. L. Pardieck, and D. J. Ziolkowski. 2013. The North American Breeding Bird Survey 1966–2011: Summary Analysis and Species Accounts. North American Fauna:1–32.

Schmitz, O. J., C. C. Wilmers, S. J. Leroux, C. E. Doughty, T. B. Atwood, M. Galetti, A. B. Davies, and S. J. Goetz. 2018. Animals and the zoogeochemistry of the carbon cycle. Science.

Smith, F. A., R. E. Elliott Smith, S. K. Lyons, and J. L. Payne. 2018. Body size downgrading of mammals over the late Quaternary. Science 360:310–313.

Terry, R. C., and R. J. Rowe. 2015. Energy flow and functional compensation in Great Basin small mammals under natural and anthropogenic environmental change. Proceedings of the National Academy of Sciences 112:9656–9661.

Thibault, K. M., E. P. White, A. H. Hurlbert, and S. K. M. Ernest. 2011. Multimodality in the individual size distributions of bird communities. Global Ecology and Biogeography 20:145–153.

Warwick, R. M., and K. R. Clarke. 1994. Relearning the ABC: Taxonomic changes and abundance/biomass relationships in disturbed benthic communities. Marine Biology 118:739–744.

White, E. P. 2004. Two-phase species–time relationships in North American land birds. Ecology Letters 7:329–336.

White, E. P., S. K. M. Ernest, A. J. Kerkhoff, and B. J. Enquist. 2007. Relationships between body size and abundance in ecology. Trends in Ecology & Evolution 22:323–330.

White, E. P., S. K. M. Ernest, and K. M. Thibault. 2004. Trade-offs in Community Properties through Time in a Desert Rodent Community. The American Naturalist 164:670–676.

Ye, H., E. K. Bledsoe, R. Diaz, S. K. M. Ernest, J. L. Simonis, E. P. White, and G. M. Yenni. 2020, May. Macroecological Analyses of Time Series Structure. Zenodo.

Yen, J. D. L., J. R. Thomson, J. M. Keith, D. M. Paganin, E. Fleishman, D. S. Dobkin, J. M. Bennett, and R. Mac Nally. 2017. Balancing generality and specificity in ecological gradient analysis with species abundance distributions and individual size distributions: Community distributions along environmental gradients. Global Ecology and Biogeography 26:318–332.

Young, H. S., D. J. McCauley, M. Galetti, and R. Dirzo. 2016. Patterns, Causes, and Consequences of Anthropocene Defaunation. Annual Review of Ecology, Evolution, and Systematics 47:333–358.